FRACTURE MECHANICS PREDICTION OF FRETTING FATIGUE UNDER CONSTANT AND VARIABLE AMPLITUDE LOADING

P.R. Edwards and R. Cook

Royal Aircraft Establishment
Farnborough
Hampshire
U.K.

Abstract

A fracture mechanics model has been developed for fretted components. It incorporates measured data on frictional forces between fretted surfaces. The model has been used with some success to predict the fatigue lives of aluminium alloy specimens with steel fretting pads having four values of slip and two values of pad load. The predictions were over a range of alternating stress levels for both constant and variable amplitude loading. This work is a step towards the analysis of a range of structural components in which fatigue failure is due to fretting with subsequent application to damage tolerant design.

1. Introduction

Fretting occurs where there is repeated movement between metal surfaces in contact. Its effect on fatigue is to speed up the initiation of fatigue cracks and it can be extremely damaging. For instance, it has been shown[1] for a clamped joint in which fatigue failure occurs in a plain aluminium alloy centre plate from the fretting action of steel side plates that the alternating stress required to cause failure in 10^7 cycles was less than one third of that for a plain aluminium alloy specimen without fretting. Similarly, fretting between a close-fitting pin or bolt and the bore of a hole in, say, a lug can be very damaging [2]. It has been suggested by a number of investigators [3-7] that the damaging effect of fretting depends upon the magnitudes of the frictional forces between fretted surfaces. In particular Endo and Goto [7] have carried out crack growth measurements on fretted specimens of mild steel. They showed that cracks initiated on shear planes (Stage 1) and then very quickly started propagating approximately normal to the surface (Stage 2) from a depth of about .03mm. There followed a period of crack growth at a rate which it was shown was highly dependent on the alternating frictional force in the fretted area. After approximately 25 percent of the life had been consumed the crack had grown away from the area over which frictional forces were being applied and it was found that frictional forces no longer affected the crack rate. Crack rates calculated from tests at a range of alternating stress levels then correlated well with the alternating stress intensity factor computed, taking into account only the alternating body stress in the specimen. Since the crack rates in the early stages of the life are dependent upon frictional forces, it seems likely that the stress intensity factor in this region contains a component which also depends upon the frictional forces. Further, the stress intensity factor at short crack lengths is also likely to contain a component which depends upon the normal fretting forces. Incorporating fretting force components into the computed stress intensity factor should enable more accurate predictions of crack rate to be made over the early part of the life in which fretting forces are significant. Although the percentage of the fretted life over which fretting forces are dominant is normally small (25 percent in the example above) it should be appreciated that were there no fretting forces the number of cycles to cover the corresponding range of crack lengths would typically be multiplied many times even if the crack would propagate at all. This suggests that fretting forces, used with an associated fracture mechanics model, could be used to predict the observed, sometimes very large, changes in life which occur when fretting conditions are varied[8].

This paper summarises the development of such a fracture mechanics model for the life prediction of fretting fatigue[9,10] and summarises the measurement of frictional forces under constant amplitude [11] and variable amplitude[12] loading. The frictional forces were required in order to scale the value of associated stress intensity factor. Also described is the application of the model to predict the lives of specimens under constant[10] and variable[13] amplitude loading. The specimens to which the model was applied were of aluminium alloy with steel fretting pads. Predictions are shown for lives obtained originally[1] under the two loading actions for four values of pad span (i.e. different values of slip) and two values of pad load. Additionally, predicted crack growth curves are compared with limited data available[14].

This work represents a stage in the development of a fracture mechanics analysis of a range of structural components in which failure is due to fretting, with subsequent application to both conventional fatigue life estimation and damage tolerant design.

2. Specimen and Material

The specimens are shown in Fig.1 together with the fretting pads. The pads were clamped to the test specimen on both sides as shown, using a steel ring and balls. The clamping force was measured by strain gauges attached to the ring and also by ring deflection. The material used for the specimen was to specification BS 2L65, being the fully artificially-aged version of a 4 percent copper-aluminium alloy. Measured tensile properties of the material are given in Table 1. The fretting pads were made from BSS98 steel. Pad spans used were 2mm, 6.35mm, 16.5mm and 34.35mm.

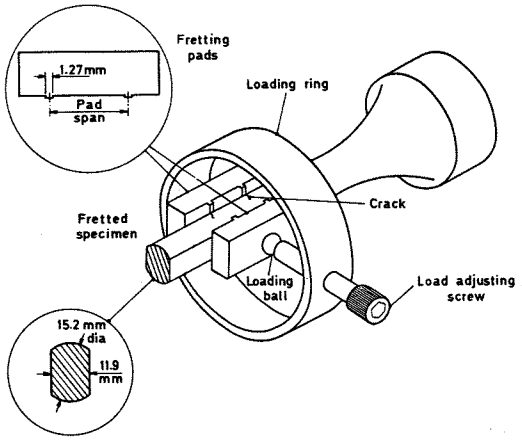

FIGURE 1: Fretted specimen assembly

0.1% Proof stress	480.6MN.m^{-2}
0.2% Proof stress	488.1MN.m^{-2}
UTS	542.4MN.m^{-2}
Elongation on 50mm G.L.	12.5%

TABLE 1
Measured mechanical properties of BS L65 aluminium alloy used in the fatigue tests(1)

3. Test Conditions

All tests were carried out at zero mean stress and at a frequency of 120Hz in a resonant fatigue machine modified(15) to apply Gaussian narrow band random loading as well as constant amplitude loading. The random loading had the form of a randomly modulated sine wave with a nominal Rayleigh distribution of peaks. This distribution was monitored and significant variations from the Rayleigh distribution were found which depended upon the magnitude of the rms stress of the waveform. One particular type of specimen was designated as "standard". This was a specimen having a pad load of 2.5kN and a pad span of 16.5mm. This was the only type of specimen which was tested as a part of both the investigations into the effect of pad span and load.

Lives to failure for the tests with four pad spans and two pad loads (2.5kN and 1.0kN) under the two loading actions are given in Section 6, where they are compared with the fracture mechanics predictions.

4. Method of Calculation of Stress Intensity Factors, Crack Rates and Lives

4.1 Stress intensity factors

The stress intensity factor at the tip of a crack growing from the end of a fretting pad was assumed to be made up from three individual contributions. First was the contribution due to the body stress in the specimen(16) and which would have been the only contribution had there been no fretting pads. Second was the contribution due to the alternating frictional loads. Both these contributions were alternating and hence damaging.

The third contribution was that due to normal pad loads. This contribution was static and compressive. Hence it tended to be beneficial. Only mode I stress intensity factors were taken into account. Although mode II (shear) stress intensity factors were present no account was taken of them as no appropriate data was available on which to base predictions.

The pad load contributions to the stress intensity factor were calculated by integrating over the fretted surface the solutions of Rooke and Jones (17) for tangential and normal line loads at a varying distance from a crack of varying length. It was assumed in all cases, as was found in practice, that the crack initiated from the front of the pad foot (the "outside" of the pad as shown in Fig.1). It was also assumed that the crack grew normal to the surface. This was not quite representative because in practice it was found that in the initial stage II crack growth the crack slanted slightly so as to grow under the pads. Since it was found that straight through cracks were common in these specimens it was assumed that the distributions of pad loads were uniform across the widths of the fretting pads. However, no such assumption could be made about the distributions of loads over the 1.27mm between the front and back of the fretting pad feet. Therefore stress intensity factors were evaluated for a range of assumed distributions of pad load as shown in Fig.2, which included the extreme cases of all the loads concentrated either at the front or back of the fretting pad foot. It was argued that the truth should lie somewhere between these two cases.

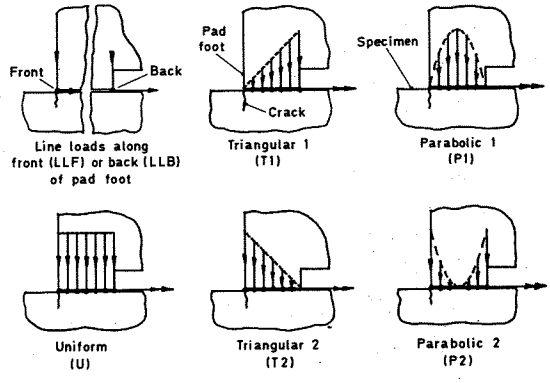

FIGURE 2: Assumed distributions of frictional and normal pad loads

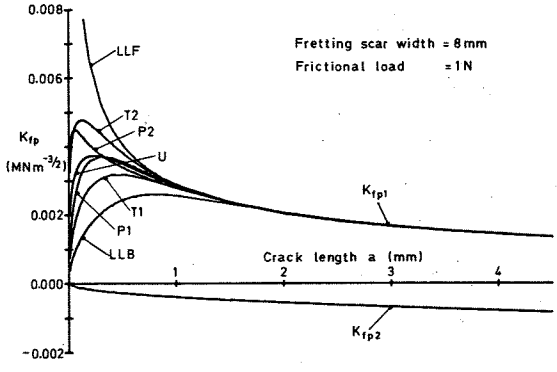

FIGURE 3: Stress intensity factors for different distributions of frictional pad load

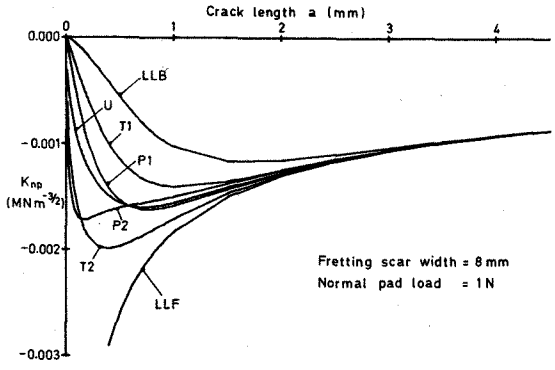

FIGURE 4: Stress intensity factors for different distributions of normal pad load

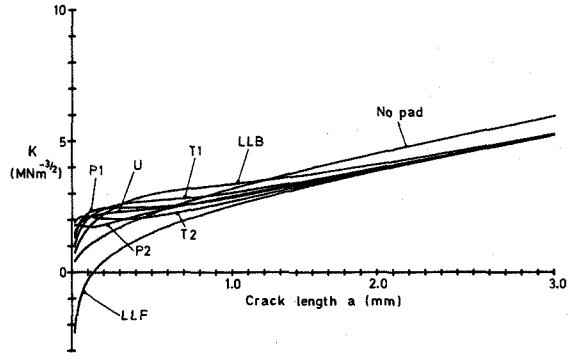

FIGURE 5: Peak stress intensity factors for a range of pad load distributions

Figs.3 and 4 show the stress intensity factors K_{fp} and K_{np} for the range of assumed pad load distributions, due to frictional and normal loads respectively assuming in each case a load of 1 Newton and a fretting scar width (the longer dimension of the fretting scar) of 8mm. As can be seen from Fig.3, the stress intensity factor due to frictional forces is split into two components, K_{fp1} which varies with the assumed pad load distribution, and K_{fp2} which is negative and accounts for the fact that the specimen alternating body stress is lower under the pads because some load is diverted through the pads. From ref 10:

$$K_{fp2} = -1.12\frac{F_f}{A}\sqrt{\pi a} \qquad (1)$$

The alternating stress intensity factor K_a is given by the components due to alternating body stress a and frictional force F_f.

$$K_a = 1.12\,\sigma_a\sqrt{\pi a} + \frac{.008}{e}F_f K_{fp1} - 1.12\frac{F_f}{A}\sqrt{\pi a} \qquad (2)$$

and the mean stress intensity factor by

$$K_m = 1.12\,\sigma_m\sqrt{\pi a} + \frac{.008}{e}F_n K_{np} + K_\ell \qquad (3)$$

where K_ℓ is the crack length correction stress intensity factor described in Section 4.3 and used in some predictions. e is the fretting scar width. The term .008/e is included in the above equations to allow for the fact that scar widths vary somewhat with fretting conditions and K_{fp1} and K_{np} apply to a scar width of 8mm.

Both mean and alternating stress intensity factors were multiplied by the finite width correction of Harris[16] for an edge crack in a specimen with the ends restrained in bending.

$$f\left(\frac{a}{w}\right) = \frac{5}{1.12\left(20-13\left(\frac{a}{w}\right)-7\left(\frac{a}{w}\right)^2\right)^{\frac{1}{2}}} \qquad (4)$$

The above finite width correction was found to be the most appropriate one to use following some residual static strength tests on part-fatigued specimens[14].

Fig.5 shows calculated peak stress intensity factors, not including the length correction K_ℓ (Section 4.3), for a standard fretted specimen under constant amplitude loading at 35MN.m^{-2} rms alternating stress. One curve is shown for each of the assumed pad load distributions and also for a specimen without pads.

As can be seen, all the fretting cases, except for assumed line loads at the front of the pad foot, show similar behaviour in that the stress intensity factor rises sharply just under the surface and then tends to level off. All the curves for fretting cases predict that, for cracks longer than about 1mm, stress intensities are lower than in the unfretted case.

Thus the fracture mechanics model is consistent with the behaviour measured by Endo and Goto[7] in that not only do fretting pads give early crack initiation. Equally important are the raised stress intensities just below the surface which enable cracks to propagate from much smaller initial flaw sizes than for plain specimens.

4.2 Calculation of crack rates

At specified values of crack length the mean stress intensity factor K_m was calculated from equation (3), together with the appropriate range of alternating stress intensity factors K_a from equation (2) corresponding to the alternating rms stress σ_r applied. Equation (2) required values of measured frictional force, interpolated where necessary, as described in Section 5. Only one value of K_a per crack length was required for constant amplitude loading. This was used together with K_m and a computer subroutine[18] to obtain the crack rate $\frac{da}{dN}$ from Pearson's[19] crack rate data for "long" $\frac{da}{dN}$ cracks (0.25mm). For variable amplitude loading, at each crack length crack rates were calculated for K_m and the range of values of K_a appropriate to the magnitude of the individual cycles in the spectrum. The final rate was obtained by a linear summation of these rates weighted according to the probability of occurrence of K_a within each variable amplitude sequence viz

$$\left(\frac{da}{dN}\right)_{random} = p(K_a)\frac{da}{dN}(K_a)\,dK_a \qquad (5)$$

Curves of crack length vs cycles were obtained by integrating numerically the inverse crack rate $\frac{dN}{da}$ along the crack length. Failure was assumed to occur when the peak stress intensity factor exceeded K_{1c} which was taken to be 27.5MN.m$^{-3/2}$ (20). As can be seen from equation (5) no allowance was made for retardation of the crack rate by high loads in the spectrum or for the difference in test frequency between that used for the crack propagation data (25Hz)and that used in the test programme (120Hz).

4.3 Use of the crack length correction

A number of predictions in this Paper were made with the crack length correction (length correction) stress intensity factor[9,10] K_ℓ included in the value of K_m. The origin of this is as follows.

Frost, Pook and Denton[21] have shown that for a range of metals at zero mean stress the stress intensity factor giving the threshold of crack propagation at short crack lengths ($a < 0.25$mm) is only about 60 percent of that for crack lengths longer than 0.5mm. Another way of expressing this is as the incompatibility between the observed empirical rule for determining the threshold of crack propagation for cracks over a range of lengths up to 4mm

$$\sigma_c^3 a = \text{const} \qquad (6)$$

and the rule expected by the application of elementary fracture mechanics is

$$\sigma_c^2 a = \text{const} \qquad (7)$$

where σ_c is the alternating stress below which the crack will not propagate.

Also Fisher and Sherratt[22] found, when monitoring crack growth from notches in mild steel specimens, that short cracks ($\approx$0.1mm) propagated considerably faster than longer cracks ($\approx$0.6mm) where the computed alternating stress intensity factor was the same in both cases.

Pook[23] has suggested that the effect can be explained by crack closure in that at short crack lengths the plastic zone at the tip of the crack is more effective at propping open the crack than at longer crack lengths. Thus at short crack lengths the effective range of stress intensity factor is greater because the crack does not close until the crack is some way into compression. The length correction stress intensity factor K_ℓ is an estimate of this extra effective range of stress intensity factor. It is given by the difference between the experimentally-determined semi-range alternating stress intensity factor for the crack length under consideration and that for long cracks. It has been computed for L65 aluminium alloy[9,10] as (MN - metre units).

$$K_\ell = 2.09 - 5.27a \quad , (a \leqslant 3.84.10^{-3}\text{m})$$

$$K_\ell = 0 \quad , (a \geqslant 3.84.10^{-3}\text{m}) \qquad (8)$$

5. Summary of Frictional Force Measurements

A series of measurements of frictional force between fretting pads and specimens was made under constant[11] and variable[12] amplitude loading. The measurements were made at the same test frequency as the rest of the tests described in this Paper, using specimens as shown in Fig.1. There were however detail differences in the fretting pads arising from the need to affix the strain gauges by means of which the frictional forces were measured. Fatigue lives achieved on specimens upon which frictional forces were measured were recorded and generally agreed reasonably well with those obtained in the rest of the test programme.

In the frictional force measurements two types of slip (or relative movement between pads and specimens) were noted confirming previous observations by Endo and co-workers[6]. The first type was termed "elastic slip". Where this occurred frictional forces were approximately proportional to slip and fretting scars were relatively superficial. Following work by O'Connor and Johnson[24] it was concluded that in this situation frictional forces were developed by elastic deformation of contacting asperities. The second type of slip was termed macro-slip, during which the frictional force was relatively independent of slip during any cycle. In this case the asperities were sliding over each and the fretting pads tended to wear away the specimen surface thus forming a groove ("keying-in"[25]).

In all the tests carried out using constant amplitude loading it was found that there was a very short initial bedding-in period of elastic slip and macro-slip, during which alternating frictional forces increased rapidly. During this period macro-slip reduced until it either ceased altogether at less than one percent of the fatigue life, or continued virtually throughout the life. In this latter situation keyed-in scars were noted and "frictional" forces tended to increase sharply at the peaks and troughs of the loading waveform, indicating that the fretting pads were coming up against the sides of the keyed-in grooves. This suggested that where macro-slip was taking place the frictional forces at the peaks and troughs of each loading cycle would tend to be concentrated at the back of each pad foot. Significant keying-in was found to occur wherever average semi-range coefficients of friction greater than .85 were recorded. Fig.6 summarises the frictional forces

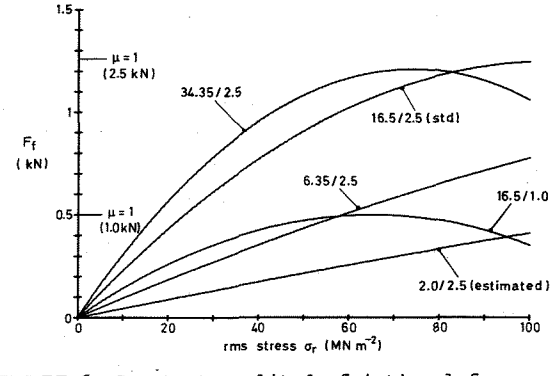

FIGURE 6: Constant amplitude frictional forces at different pad spans (mm)/pad loads (kN)

measured under constant amplitude loading. As can be seen, for the specimens with a pad load of 2.5kN it was found that average frictional forces generally increased with increasing pad span due to the action of elastic slip. However, at the higher alternating stress levels on specimens with the two longest pad spans substantial macro-slip occurred and frictional forces peaked at a coefficient of friction of approximately unity. On specimens with the low pad load, frictional forces also peaked at a coefficient of friction of approximately unity. It should be noted that this represented only 40 percent of the maximum frictional forces recorded at the higher pad load.

Under variable amplitude loading each loading sequence contained a range of component alternating stresses each with its associated range of alternating frictional force values and these were monitored simultaneously. Thus for any variable amplitude test a curve of the type shown in Fig.6 could be constructed which applied to the component cycles. This curve was not in general the same as that obtained under constant amplitude loading for specimens with the same pad load and span, and in some cases different curves were obtained for different rms values of variable amplitude stress on specimens with the same pad load and span. This difference was associated with the bedding-in process, which, under constant amplitude loading rapidly increased the frictional force value at which macro-slip occurred and hence the maximum frictional force. Under variable amplitude loading however, the bedding-in process was continually disturbed by groups of higher level cycles which reduced the frictional force at which macro-slip occurred. The bedding-in would then start again. The outcome of this was that keying-in was much more marked under variable amplitude loading. Also the steady state frictional forces measured under constant amplitude loading tended to be upper bounds for the values measured at component cycles in variable amplitude sequences. This is shown in Fig.7 which compares frictional forces measured for standard fretted specimens under variable amplitude loading at three rms stress levels with those recorded in the constant amplitude tests. Because of the continual changes in frictional force at which macro-slip occurred there was considerable scatter in measured frictional forces at the higher component rms levels. However, as can be seen, there was little variation with random rms level of the average curves.

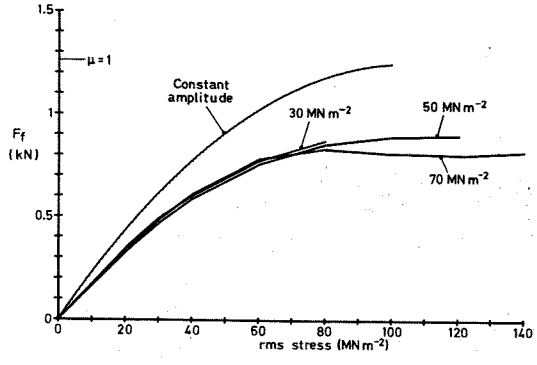

FIGURE 7: Frictional forces on standard fretted specimens - constant & variable amplitude loading

Fig.8 compares frictional forces under the two types of loading for specimens with the same pad load as above but with the longer pad span of 34.35mm. As can be seen on these specimens which showed the largest amount of macro-slip of any tested, there was a marked difference between the frictional forces at the three random rms levels. Also frictional forces measured at the lower component alternating stress levels were similar to those under constant amplitude loading. Similar relative behaviour of frictional forces under the two loading actions was found for specimens with the low pad load.

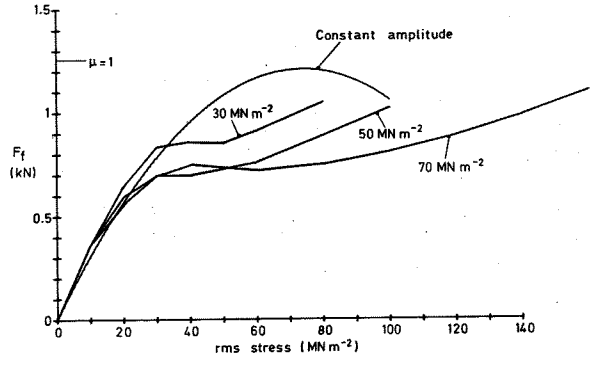

FIGURE 8: Frictional forces for constant and variable amplitude loading - pad span = 34.35mm load = 2.5kN

Specimens with a pad span of 6.35mm and a pad load of 2.5kN showed frictional forces consistently about 70 percent of those recorded under constant amplitude loading.

Thus it can be seen that there was no simple relationship between frictional forces and component alternating stresses within variable amplitude loading sequences. The relationship changed with the random rms alternating stress as well as with pad load and span. Therefore when applying equation (2) in the fracture mechanics predictions, frictional forces were obtained by interpolating the appropriate measured values. Where frictional forces were required for random rms levels higher than 70MN.m^{-2} or lower than 30MN.m^{-2} the values for 70MN.m^{-2} or 30MN.m^{-2} respectively were assumed.

6. Fracture Mechanics Predictions

Pad Load (kN)	Span (mm)	Scar Widths	
		Constant Amplitude (mm)	Gaussian Random (mm)
2.5	34.35	8.0	9.5
2.5	16.50	8.0	8.1
2.5	6.35	8.0	8.5
2.5	2.00	8.0	8.1
1.0	16.50	5.6	7.0

TABLE 2 Widths of fretting scars

All the stress intensity factors used for the prediction described in this section were computed assuming fretting scar widths as in Table 2. It was assumed in all cases that the distribution

of normal loads had the same shape as the distribution of frictional loads.

6.1 Effect of initial flaw size and length correction on predicted life

All fracture mechanics analyses have to assume an initial flaw size from which the crack propagates. Examination of the fracture surfaces of the fretted specimens showed that by the time cracks had reached a depth of .02mm, the majority were propagating in a stage 2 manner, except that they tended to slant slightly so as to grow under the fretting pads.

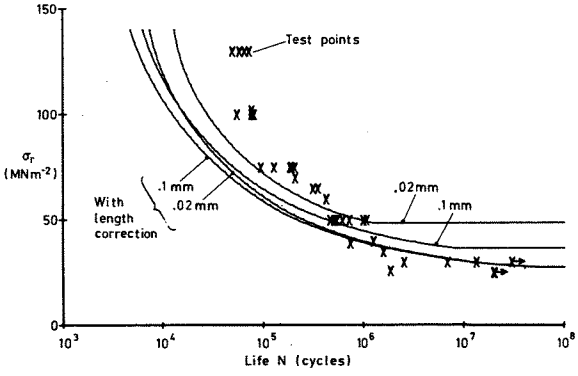

FIGURE 9: Effect of initial flaw size on predicted life - constant amplitude loading

Fig.9 compares experimentally achieved lives of standard fretted specimens under constant amplitude loading with those predicted assuming uniform pad load distributions and initial flaw sizes of .02 and 0.1mm with and without the length correction. Considering first the predictions without the length correction, these were less than satisfactory in two respects. First the predicted curves were too "flat". At the higher stress levels predicted lives were too short and at the lower stress levels they were too long. Also the predicted fatigue limits were due to the initial flaw not propagating, whereas experimental evidence[1] was that the fatigue limit was due to cracks stopping at around 0.2mm. Considering now the predictions using the length correction, it can be seen that the fatigue limit was predicted very much better and in fact the predicted fatigue limit was this time due to cracks stopping after an initial period of propagation. Also, the predicted curve was steeper than without the length correction, which was also an improvement. However, at the highest stress levels the predicted lives were too short by a large factor.

Figs.10 and 11 show the effect of initial flaw size on the predicted life of standard fretted specimens under variable amplitude loading without and with the length correction respectively. Uniform pad load distributions were assumed. A comparison with Fig.9 shows that the variable amplitude predictions were more accurate than the corresponding constant amplitude predictions. As before the predictions without the length correction gave an S-N curve that was too flat and the use of the length correction gave predictions that were more accurate at the lower stress levels but predicted lives that were too short at the higher stress levels. However, the difference between predictions with and without the length correction was not as marked as for constant amplitude loading.

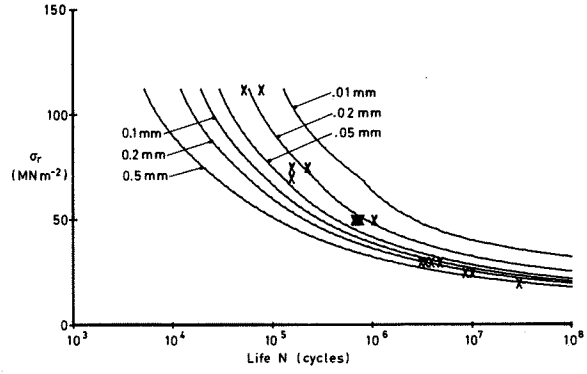

FIGURE 10: Effect of initial flaw size on predicted life - variable amplitude - no length correction

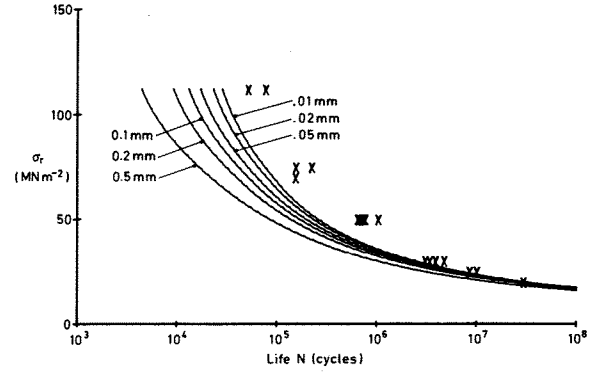

FIGURE 11: Effect of initial flaw size on predicted life - variable amplitude - length correction used

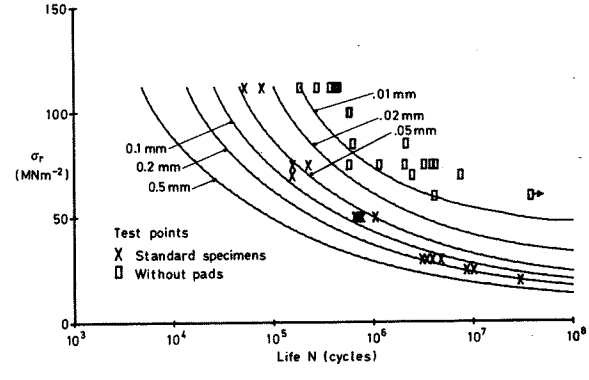

FIGURE 12: Effect of initial flaw size on predicted life - no pads - variable amplitude - length correction used

Fig.12 shows predicted variable amplitude S-N curves for plain specimens assuming a range of initial flaw sizes and using the length correction.

Experimental test points for standard fretted and plain specimens are shown for reference. Comparison with the equivalent predictions for standard fretted specimens (Fig.11) shows that in the latter case the effect of initial flaw size was far less marked. The reason for this less critical behaviour for specimens with pads was that in this case the stress intensity factor, and hence the crack rate, was more nearly constant over the fatigue life (Fig.5). The same was found to apply for constant amplitude loading.

Summarising the effect of initial flaw size on predicted fatigue life, it was found that it was not nearly as large for fretted as for unfretted specimens. The use of the length correction greatly improved predictions under both constant and variable amplitude loading close to the fatigue limit and also predicted the observed fact that the fatigue limit was due to cracks stopping after an initial period of propagation. However, the accuracy of prediction at the higher stress levels was worse with the length correction, particularly for constant amplitude loading.

6.2 Predicted and measured crack propagation curves

Figs.13 and 14 show predicted crack propagation curves for constant and variable amplitude loading on standard fretted specimens. In both cases a uniform distribution of pad loads was assumed with an initial flaw size of .02mm, and crack lengths were plotted against fraction of life consumed so that the shapes of the crack propagation curves could be compared at different stress levels. As can be seen, in both these figures the predictions, in which the length correction was used, varied markedly in shape with alternating stress level. Similar sets of curves for both loading actions, constructed without using the length correction, were found not to vary very much in shape with stress level. One curve predicted without the length correction is plotted for each loading action for an rms stress level of 50MN.m^{-2} and is labelled "NLC". Finally, a measured crack propagation curve for each loading action at an rms stress of 50MN.m^{-2} is plotted in Figs.13 and 14. These curves were constructed by fatigue testing specimens to different percentages of the expected life to failure, breaking them statically and measuring the sizes of any fatigue cracks thus revealed[14].

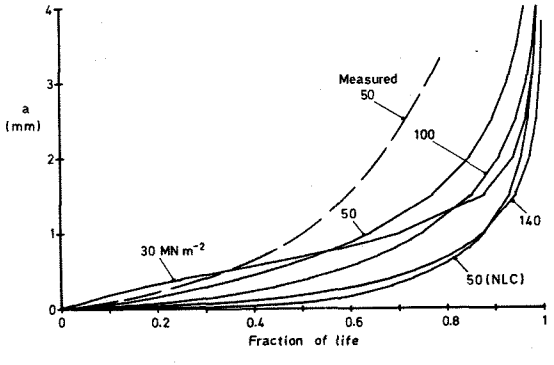

FIGURE 13: Predicted and measured curves - constant amplitude loading

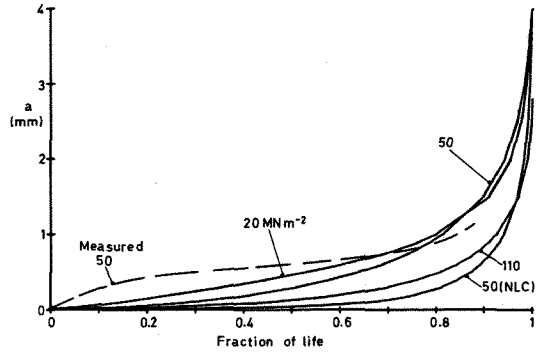

FIGURE 14: Predicted and measured curves - variable amplitude loading

As can be seen from Fig.13, the measured curve for constant amplitude loading agreed rather better with that predicted using the length correction than that without. Also, further similar measurements indicated that at 30MN.m^{-2} rms cracks of 0.2mm commonly existed at 5 percent of the life whereas at 62.5MN.m^{-2} the corresponding crack length was .06mm. As can be seen from Fig.13 although the predicted crack lengths at 5 percent of the life were not as long as the measured values above, the predicted curves using the length correction were more nearly in accordance with the measurements in that at the lower stress levels the crack reached any particular length at a much earlier percentage of the life than at the higher stress levels.

For the case of variable amplitude loading it can be seen that although the prediction using the length correction gave better agreement with the measured curve than that without, the agreement was not good. In particular, neither of the predictions indicated the observed fact that the crack curve would start off at a relatively fast rate and then slow down. The overall shape of the measured curve was confirmed in other work. Standard fretted specimens were subjected to tests in which the fretting pads were removed at different stages in the life [1] and the tests continued to failure. It was found that under constant amplitude loading over a range of stress levels, removing the pads at up to 30 percent of the life gave an increase in the life. However, for variable amplitude loading the corresponding value was 5 percent. This difference in behaviour is explicable if it is accepted that under variable amplitude loading, but not under constant amplitude loading, fatigue cracks propagate relatively fast out of the region in which pad loads give a big contribution to the stress intensity factor and then slow down. A second piece of evidence confirming the shapes of the measured crack propagation curves involved acoustic emission traces obtained on standard fretted specimens under both types of loading[14]. Under variable amplitude loading it was found that there was an initial period of acoustic emission activity which could have been associated with an early period of relatively fast crack growth. This was not found for constant amplitude loading.

Thus it can be seen that three separate pieces of evidence confirm that under variable amplitude loading the shape of the crack propagation curve

was markedly different to that under constant amplitude loading. It would appear that in these specimens a fracture mechanics model which was reasonably accurate in predicting the shape of the crack propagation curve under constant amplitude loading was very inaccurate under variable amplitude loading. Therefore either the stress intensity factors calculated for variable amplitude loading were much less accurate than for constant amplitude loading or the cumulative damage model used was inaccurate. As described in Section 4.2, the cumulative damage model used was a linear summation of constant amplitude crack rates weighted according to the probabilities of occurrence of alternating stress intensity factors within each variable amplitude sequence.

On the first possibility for error, as described in Section 4, account was taken of the main parameter which governs the magnitude of the stress intensity factor under fretting conditions, the frictional forces. It was thought that these could well be different under variable amplitude loading as in fact was the case (Section 5). Stress intensity factors were calculated using values measured under variable amplitude loading. However, although the resulting distributions of stress intensity factor gave predicted lives significantly different from those assuming the same frictional forces as under constant amplitude loading, the shapes of the distributions of stress intensity factor were similar to those used before. Also the shapes of crack propagation curves predicted in Figs.13 and 14 were similar. The only way that frictional forces could have explained the observed crack propagation curve for variable amplitude loading would have been if they had reduced drastically over the early part of the life. This was not found to be the case. An assessment of other parameters known to affect the magnitude of the stress intensity factor, e.g. pad load distribution, did not reveal any which would be capable of changing sufficiently under variable amplitude loading to account for the effect.

The other possible explanation for the unusual shape of crack propagation curve is that the cumulative damage model was not adequate. It is known that under variable amplitude loading the linear summation model used in this report normally predicts crack rates which are too fast. This has been attributed[26] to premature crack closure following the application of high loads in sequence. However, very little is known about crack propagation at short crack lengths. As discussed in Section 4.4, faster than expected crack rates at short crack lengths under constant amplitude loading have been attributed to a large difference between crack closure behaviour at short crack lengths and closure at long crack lengths. It is possible therefore that the cumulative damage behaviour in crack propagation may be different at short crack lengths in the region where a relatively accelerated growth rate was measured under variable amplitude loading.

Thus although the shape of the crack propagation curve was predicted better using the length correction than not using it, there were still substantial errors in the prediction. More work involving the measurement of cracks under constant and variable amplitude loading is necessary to establish the scope and magnitude of these errors and their cause. If these errors are shown to be widespread and as large as indicated by the limited data obtained at 50MN.m^{-2}, then the fracture mechanics model will need some modification.

6.3 Effect of assumed distributions of pad load on fatigue life

As was shown in Sections 6.1 and 6.2, the predictions using the length correction described better the crack propagation behaviour of the fretted specimens, particularly for constant amplitude loading. Because of this, the remainder of the predictions presented in this paper were carried out using the length correction. A more extensive assessment of the length correction is given in Refs.10 and 13.

As described in Section 6.1, the most inaccurate predictions made for standard fretted specimens assuming a uniform distribution of pad loads were under constant amplitude loading at the highest stress levels. However, there was some evidence (Section 5) that frictional forces under these conditions were concentrated towards the back of the fretting pad foot, since it appeared that they arose from pad feet running into lines of debris or the edges of keyed-in grooves. This only happened at stresses above 70MN.m^{-2}, where keying-in was taking place. Fig.15 shows predicted and achieved lives for standard fretted specimens under constant amplitude loading with an assumed initial flaw size of .02mm and a range of assumed pad load distributions. As can be seen, all the distributions which were symmetrical about the middle of the fretting pad foot predicted lives that were similar to those for uniform pad load distributions. It can also be seen that the assumption of distributions where the pad loads were more concentrated towards the back of the pad foot improved predictions at the higher stress levels. However, even with all the loads concentrated at the back of the pad foot, the predicted lives at the highest levels were still too short.

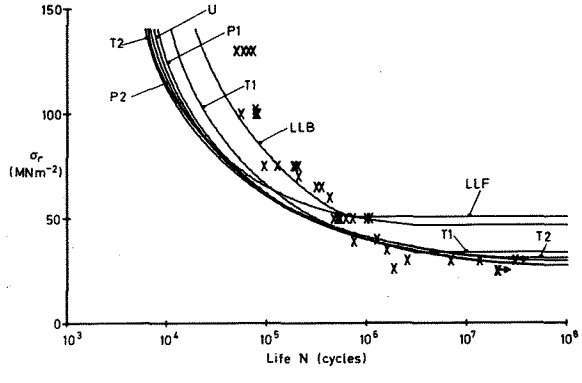

FIGURE 15: Predicted lives for a range of pad load distributions - constant amplitude

The predicted curve assuming line loads at the front of the pad foot can be seen from Fig.15 to have a rather different shape to the others. Although not obvious from the predictions shown in this Paper, the above assumption predicted some extreme changes in life as frictional and normal forces were varied. This was due to the fact that

for this pad load distribution both the frictional and normal contributions to the stress intensity factor tended to infinity as zero crack length was approached (Figs.3 and 4). Thus the stress intensity factor at short crack lengths was primarily the result of two large components that tended to oppose each other and a small percentage change in one component could give a large change in the resultant stress intensity factor. This extreme behaviour was not found for the other assumed pad load distributions which, as discussed above, were more likely to apply in practice.

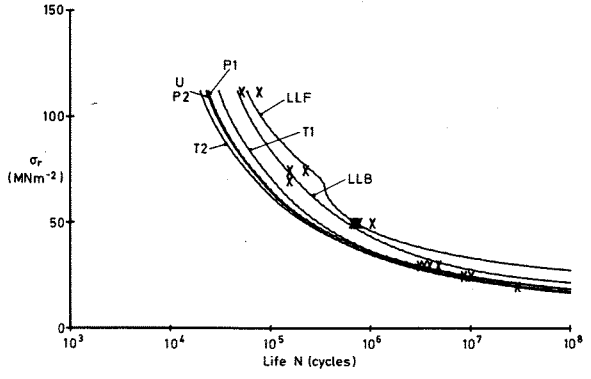

FIGURE 16: Predicted lives for a range of pad load distributions - variable amplitude

Fig.16 shows the same set of predictions as for Fig.15, except that Fig.16 applies to variable amplitude loading. It can be seen that apart from the curve assuming a line load at the front of the pad foot (see above), the pattern of predictions was similar to that under constant amplitude loading. However, particularly at the higher stress levels, the predictions tended to be more accurate. Under variable amplitude loading keying-in occurred at all stress levels on the standard fretted specimens. Under these conditions the sudden build up in "frictional forces" at the waveform peaks and troughs was evident, as for constant amplitude loading (Section 5), but was not as marked and only occurred at the higher level cycles within the sequence, presumably because only these cycles deflected the specimen enough for the pad feet to approach the sides of the keyed-in groove. Thus some tendency would be expected for the pad loads at the peaks of the stress cycles to concentrate towards the back of the pad foot, but not to the same extent as under constant amplitude loading. The most appropriate predicted curve would be expected to be between triangular 1 and the left hand group of curves representing symmetrical distributions. This would still give variable amplitude predictions that were rather more accurate than those for constant amplitude loading. However, two more factors would be expected to improve the variable amplitude predictions further.

First, in the variable amplitude case the frictional forces assumed for rms stresses above 70MN.m^{-2} were those measured at that level (Fig.7). Had the fatigue machine on which the measurements were made been able to apply stresses above this level, it is likely that lower frictional forces would have been recorded (cf.Fig.8) and predicted lives would have been longer. Second, allowance for retardation of the crack due to high loads in the sequence[27] would have further increased predicted life.

Thus variable amplitude predictions particularly taking into account the additional factors described above were more accurate than the corresponding constant amplitude predictions. This was a rather surprising result in view of the errors indicated by a comparison of predicted and measured crack curves in Section 6.2.

6.4 Predictions for a range of pad spans

Figs.17 and 18 show predictions for the two loading actions applied to specimens having the full range of pad spans at a pad load of 2.5kN. The predictions were all made on the same basis, i.e. using the length correction, an initial flaw size of .02mm and triangular 1 pad load distributions. As discussed in Section 6.3, there was some evidence that distributions of pad load varied depending on the fretting conditions and taking account of this would be expected to improve the predictions. However, the assumption of triangular 1 pad load distribution can be regarded as a reasonable compromise to illustrate the way that the model predicts the effect of pad span on fatigue life.

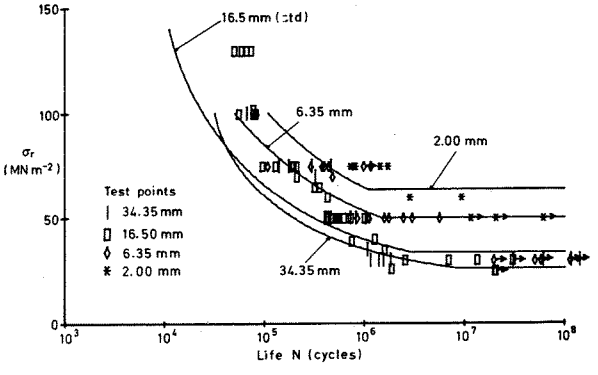

FIGURE 17: Predicted and achieved lives for a range of pad spans - constant amplitude

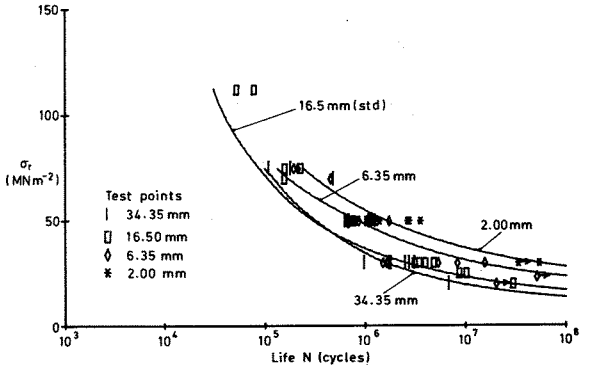

FIGURE 18: Predicted and achieved lives for a range of pad spans - variable amplitude

As can be seen from Figs.17 and 18, the relative variation of fatigue life with pad span was predicted very well for constant and variable amplitude loading respectively. This predicted variation in life with pad span was due entirely to the associated changes in frictional force and the related stress intensity factor. Predicted lives were consistently more accurate under variable amplitude loading.

6.5 Predictions at two pad loads

Fig.19 shows experimental and predicted lives for specimens with a pad span of 16.5mm and two values of pad load, 1kN and 2.5kN under constant amplitude loading. Fig.20 shows the same for variable amplitude loading. Predictions were made making the same assumptions as to initial flaw size etc. as described in Section 6.4. As can be seen, the relative effect of changing the pad load was predicted well for both constant and variable amplitude loading. As before the most accurate life predictions were for variable amplitude loading. The effect of pad load on predicted and achieved fatigue life was small at the lower stress levels as can be seen for both constant (Fig.19) and variable (Fig.20) amplitude loading. This may appear to be rather surprising at first sight in view of the relatively large differences in frictional force recorded between the two pad loads (Section 5). However, there were two factors which offset this. First the fretting scar width was less at the low pad load (Table 2). Much more important was the fact that reducing the normal pad load reduced the magnitude of its associated beneficial stress intensity factor. This tended to offset the reduction in the damaging stress intensity factor associated with the frictional loads. The net effect was that predicted lives could go up or down with pad load. As can be seen from Fig.19 at different stress levels it was predicted that the life would generally increase with decrease in pad load, except over a small range of alternating rms stresses around 40MN.m^{-2} where a small decrease was predicted.

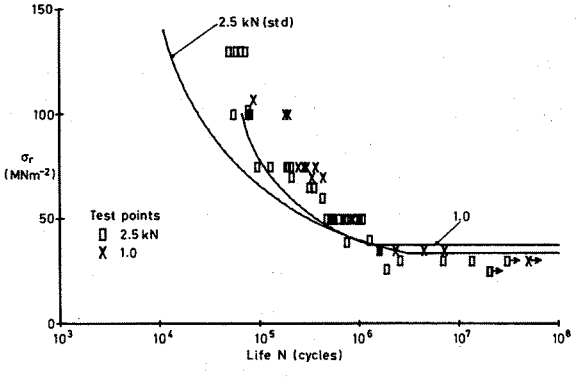

FIGURE 19: Predicted and achieved lives for two pad loads - pad span = 16.5mm - constant amplitude

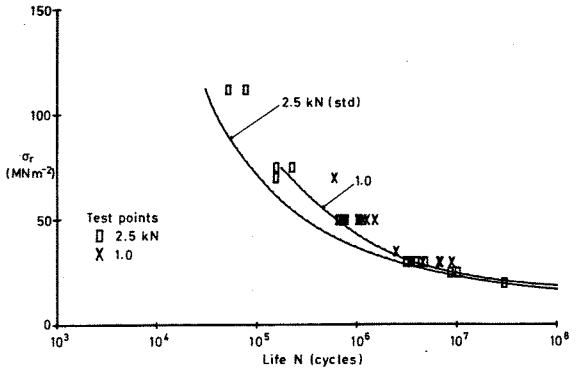

FIGURE 20: Predicted and achieved lives for two pad loads - pad span = 16.5mm - variable amplitude

7. Concluding Discussion

It was considered that the accuracy of the predictions under both constant and variable loading was very good considering the possible sources of error. There were some large errors in predicted lives at the higher stress levels under constant amplitude loading but these may well be reduced considerably as the model is refined to account for the sources of error listed below. Particularly encouraging was the way in which the model predicted the effect on life of varying the pad span and pad load for both constant and variable amplitude loading, and predicted shapes of crack propagation curves under constant amplitude loading which agreed well with limited available measured data. It is considered that the most serious deficiency in the model was its failure to predict the observed fact that under variable amplitude loading the crack propagated initially at a relatively fast rate and then slowed down. This is discussed in detail in Section 6.2. Possible sources of error which apply to predictions under both constant and variable amplitude loading are listed below:

1. Crack rate data for crack rates below about 3 x 10^{-5}mm/cycle is very scarce and numerical data defining the behaviour of cracks at lengths well below 1mm is even scarcer. Pearson's data[19], which was used in this Paper and assessed as the best available, covered a range of crack rates down to about 3 x 10^{-6}mm/cycle and was thereafter extrapolated over more than two decades of crack propagation rate down to the threshold value measured by Frost[21] about 18 years ago. As discussed in Section 4.2, crack propagation in the region of this extrapolation is not well understood. Therefore, since large proportions of the predicted lives in this Paper were calculated at short crack lengths with stress intensities close to the threshold of crack propagation, substantial errors were possible. The length correction was used in this Paper in an attempt to account for anomalous behaviour at short cracks and on the whole improved predictions, but it should be emphasised that it was based on limited data.

2. It is to be expected that local variations in the normal and frictional loads under the pad would lead to local variations of stress intensity factor close to the surface and locally affect crack propagation rates at short crack lengths.

3. Multiple cracks were present on many of the fretted specimens, particularly those in the keying-in situation and would tend to slow crack rates where one crack was shielding another.

4. Mode II stress intensity factors were present due to both normal and frictional pad loads and were not taken into account, due to lack of appropriate crack propagation data. Neither was the fact that cracks tended to propagate initially at an angle so as to grow under the pads.

5. No allowance was made for the difference in frequency between that at which the crack rate data was obtained (25Hz) and that at which the fretting tests were carried out (120Hz). However, available data on similar material[28] suggests that if frequency were accounted for, predicted lives could be increased by a factor of between 1.2 and 2.

6. It was assumed in all cases that the distributions of normal and frictional pad loads were the same. This may not have been the case, particularly when pads were keying-in. Also pad load distributions could change throughout the life again particularly when keying-in was occurring. Nevertheless, it should be remembered that the effect on life of pad load distribution was surprisingly small.

8. Further Work

1. Frictional force measurements and associated fatigue tests are continuing under a range of conditions including ranges of frequency and mean stress. The case of changes in mean stress is an interesting one because different fretted components and materials can show widely varying changes in life with change in mean stress[29]. The fracture mechanics model is potentially capable of explaining many of these as follows. When the mean body stress in a component changes the associated stress intensity factor also shows an increase in mean value. However, the stress intensity factors associated with the fretting forces do not change with mean stress. Therefore, the model predicts that the early part of the life which is dominated by the fretting force components is little affected by the mean stress. Thus components with different combinations of fretting forces and body stress show different sensitivity to mean stresses.

2. It is intended to carry out crack propagation measurements at short crack lengths in specimens without fretting. The specimens will be subjected to constant and variable amplitude loading. It is hoped that an improved definition of cumulative damage behaviour in crack propagation at short crack lengths will lead to a better understanding of fretting.

9. Conclusions

1. A fracture mechanics analysis of aluminium alloy specimens with steel fretting pads, subjected to constant and variable amplitude loading at zero mean stress has been carried out. Using measured data on frictional forces between the fretting pads and the specimens, predictions of fatigue lives were made for specimens having four different values of pad span (different values of slip) and two values of pad load.

2. The accuracy of predicted lives was good, particularly for variable amplitude loading. The most inaccurate predictions were made for constant amplitude loading at the highest alternating stresses. The effect on fatigue life of changing pad span and load was predicted well.

3. A crack length correction was assessed which empirically took account of the fact that short cracks having the same alternating stress intensity factor as long cracks tend to propagate faster. It was found that the use of the length correction gave very good predictions of the fatigue limits, and, overall, gave the best predicted S-N curve shapes. It also gave predicted crack propagation curves which best agreed with measured data.

4. The most serious failure of the fracture mechanics model was that it failed to predict the observed fact that under variable amplitude loading there was an initial relatively fast rate of crack propagation after which it slowed down.

List of Symbols

a	Crack length
A	Cross sectional area of specimen
e	Fretting scar width
F_f	Maximum frictional force in stress cycle on each pad foot
F_n	Normal force on each pad foot
K	Stress intensity factor
K_a	Plane strain fracture toughness
K_ℓ	Length correction stress intensity factor
K_m	Mean stress intensity factor
K_{fp}	Stress intensity factor due to frictional load of 1N on fretting scar of width 8mm
K_{fp1}	As K_{fp} but without component due to reacting stresses
K_{fp2}	Component of K_{fp} due to reacting stresses
K_{np}	Stress intensity factor due to normal load of 1N on fretting scar width of 8mm
K_{1c}	Plane strain fracture toughness
N	Number of cycles to failure
$p(K_a)$	Probability distribution of K_a

List of Symbols (continued)

w	Distance between fretted surfaces (specimen depth)
σ_a	Semi-range alternating body stress in specimen
σ_c	Semi-range alternating body stress in specimen to give threshold of crack propagation
σ_m	Mean body stress
σ_r	rms alternating stress
μ	Coefficient of friction

References

1 P.R.Edwards, R.J.Ryman
Studies in fretting fatigue under service loading conditions.
Proc. Eighth ICAF Symposium Lausanne (1975)
also RAE TR 75123 (1975)

2 P.R. Edwards
Cumulative damage in fatigue with particular reference to the effects of residual stresses.
RAE TR 69237 (1969)
(ARC C.P. 1185) (1969)

3 W.D.Milestone, J.D.Janeczko
Friction between steel surfaces during fretting.
Wear 18,29-40 (1971)

4 M.H.Wharton, R.B.Waterhouse, K.Hirakawa, K.Nishoika
The effect of different contact materials on the fretting fatigue strength of an aluminium alloy.
Wear 26, 253-260 (1973)

5 K.Endo, H.Goto, T.Nakamura
Fretting fatigue strength of several materials combinations.
Bull. JSME Vol.17, No.92 (1973)

6 K.Endo, H.Goto, T.Fukunaga
Behaviours of frictional force in fretting fatigue.
Bull. JSME Vol.17, No.108 (1974)

7 K.Endo, H.Goto
Initiation and propagation of fretting fatigue cracks.
Wear 38, 311-324 (1975)

8 A.J.Fenner, J.E.Field
Fatigue under fretting conditions.
NEL.ABDiv.16/57 (1957)

9 P.R.Edwards, R.J.Ryman, R.Cook
Fracture mechanics prediction of fretting fatigue.
Proc. Ninth ICAF Symposium Darmstadt (1977)

10 P.R.Edwards, R.J.Ryman, R.Cook
Fracture mechanics prediction of fretting fatigue under constant amplitude loading.
RAE TR 77056 (1977)

11 P.R.Edwards, R.Cook
Frictional force measurements on fretted specimens under constant amplitude loading.
RAE TR 78019 (1978)

12 P.R.Edwards, R.Cook
Frictional force measurements on fretted specimens under variable amplitude loading.
RAE TR 78059 (1978)

13 P.R.Edwards, R.Cook
Fracture mechanics prediction of fretting fatigue under Gaussian random loading.
RAE TR to be published

14 R.J.Ryman, M.P.Blackwell
An acoustic emission investigation of the initiation and propagation of fretting fatigue cracks in BS L65 aluminium alloy under constant and random amplitude loading.
Testwell Ltd. Report FAT/130 Issue 2(1978)

15 P.R.Edwards
A controller for random and constant amplitude loading on resonant and electrohydraulic fatigue machines.
RAE TR 66023 (1966)

16 D.P.Rooke, D.J.Cartwright
Compendium of stress intensity factors.
HMSO (1974)

17 D.P.Rooke, D.A.Jones
Stress intensity factors in fretting fatigue
RAE TR 77181 (1977)

18 P.R.Edwards
A computer program for the interpolation and extrapolation of crack propagation data.
RAE TR 76115 (1976)
(ARC CP 1387, 1977)

19 S.Pearson
Initiation of fatigue cracks in commercial aluminium alloys and the subsequent propagation of very small cracks.
RAE TR 72236 (1972)

20 S.Pearson
Fatigue crack initiation and propagation in half inch (12.7mm) thick specimens of aluminium alloy.
RAE TR 71109 (1971)

21 N.E.Frost, L.P.Pook, K.Denton
A fracture mechanics analysis of fatigue crack growth data for various materials.
NEL/A2/1/69 (1969)

22 B.C.Fisher, F.Sherratt
A fracture mechanics analysis of fatigue crack growth data for short cracks.
Fracture Mechanics in Engineering Practice
Applied Science Publishers (1977)

23 L.P.Pook
Various aspects of the fatigue damage threshold in mild steel.
Proc.SEE Conference "Fatigue Testing and Design" London (1976)

24 J.J.O'Connor, K.L.Johnson
The role of surface asperities in transmitting tangential forces between metals.
Wear 6, 118-139 (1963)

25 J.E.Field, D.M. Walters
Fretting fatigue strength of EN26 steel. Effects of mean stress, slip and clamping conditions.
NEL Report 275 (1967)

26 W.Elber
Fatigue crack closure under cyclic tension.
J.Eng.Frac.Mech. 2, 37-45 (1970)

27 K.O.Sippel, D.Weisgerber
Flight by flight crack propagation test results with several load aspects and comparison with calculation according to different models.
Proc.Ninth ICAF Symposium Darmstadt (1977)

28 A.Hartman, J.Schijve
The effects of environment and load frequency on the crack propagation law for macro fatigue crack growth in aluminium alloys.
Engineering Fracture Mechanics 1, 615-631 (1970)

29 B.H.E.Perrett
Fatigue endurance of structural elements in various materials under constant and variable amplitude loadings.
RAE TR 77162 (1977)